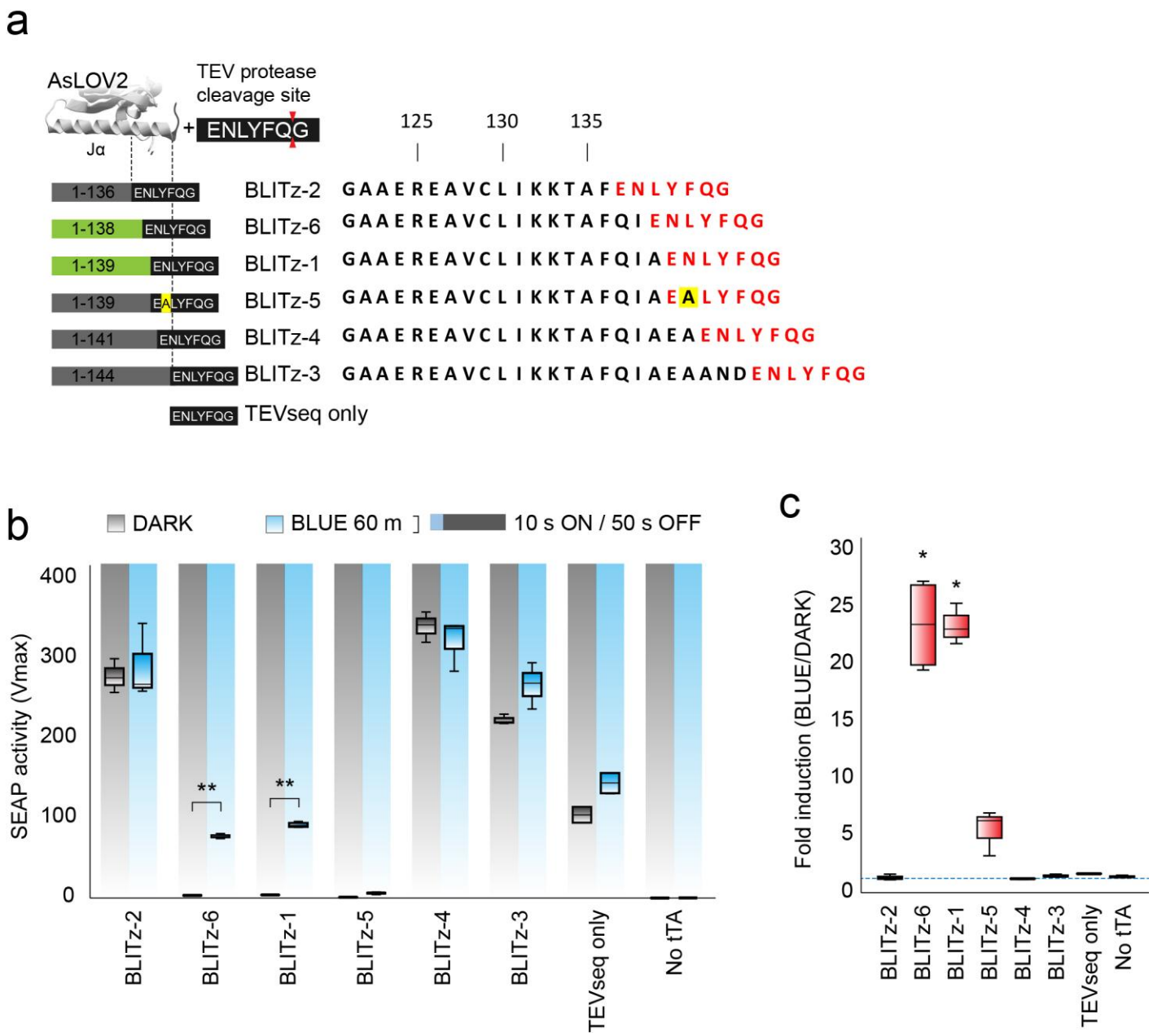

Supplementary Figure 1

Serial deletion mutants of BLITz.

(a) Design of TEVseq insertion into Jα-helix. C-terminal end of Jα-helix was serially deleted and replaced by TEVseq. TEV cleavage site is labeled as red arrowheads. Note that numbering of different BLITz is independent of deletion length. (b) Average of SEAP activity assay when transfected with different types of BLITz constructs (Dark and Blue: BLITz-2: 268.9 ± 20.5, 281.1 ± 45.2, BLITz-6: 2.21 ± 0.28, 100.7 ± 4.95, BLITz-1: 5.47 ± 0.66, 131.3 ± 5.09, BLITz-5: 1.19 ± 0.20, 5.94 ± 1.61, BLITz-4: 329.5 ± 18.4, 311.6 ± 31.6, BLITz-3: 216.1 ± 6.13, 258.4 ± 28.1, TEVseq only: 85.0 ± 7.39, 97.7 ± 3.86, No tTA: 0.29 ± 0.08, 0.34 ± 0.12). Three independent cultures were performed for each condition. DNA constructs were transfected into HEK293T cells by calcium phosphate methods. We found that the background levels of gene expression were

very high when TEVseq was inserted close to the Jα-helix C-terminus (BLITz-3 and -4), indicating that TEVseq was accessible to TEV protease. Removing two more amino acids from Jα-helix (BLITz-1 and -6), completely abolished baseline gene expression, while maintaining high light-induced gene expression. Interestingly, removing amino acids 137 and 138 (BLITz-2) restored the baseline gene expression, suggesting those amino acids are tied to the light-dependent conformational changes. We subsequently tested intact TEVseq without fusion to AsLOV2 protein (similar to classical Tango system) and observed that basal gene expression was high, as expected, and subsequent fold change was minimal (~1.4 fold). Removal of TetR-VP16 (No tTA) led to nearly undetectable signals, suggesting that background gene expression did not originate from the reporter itself. (c) Fold induction changes when blue light was illuminated.

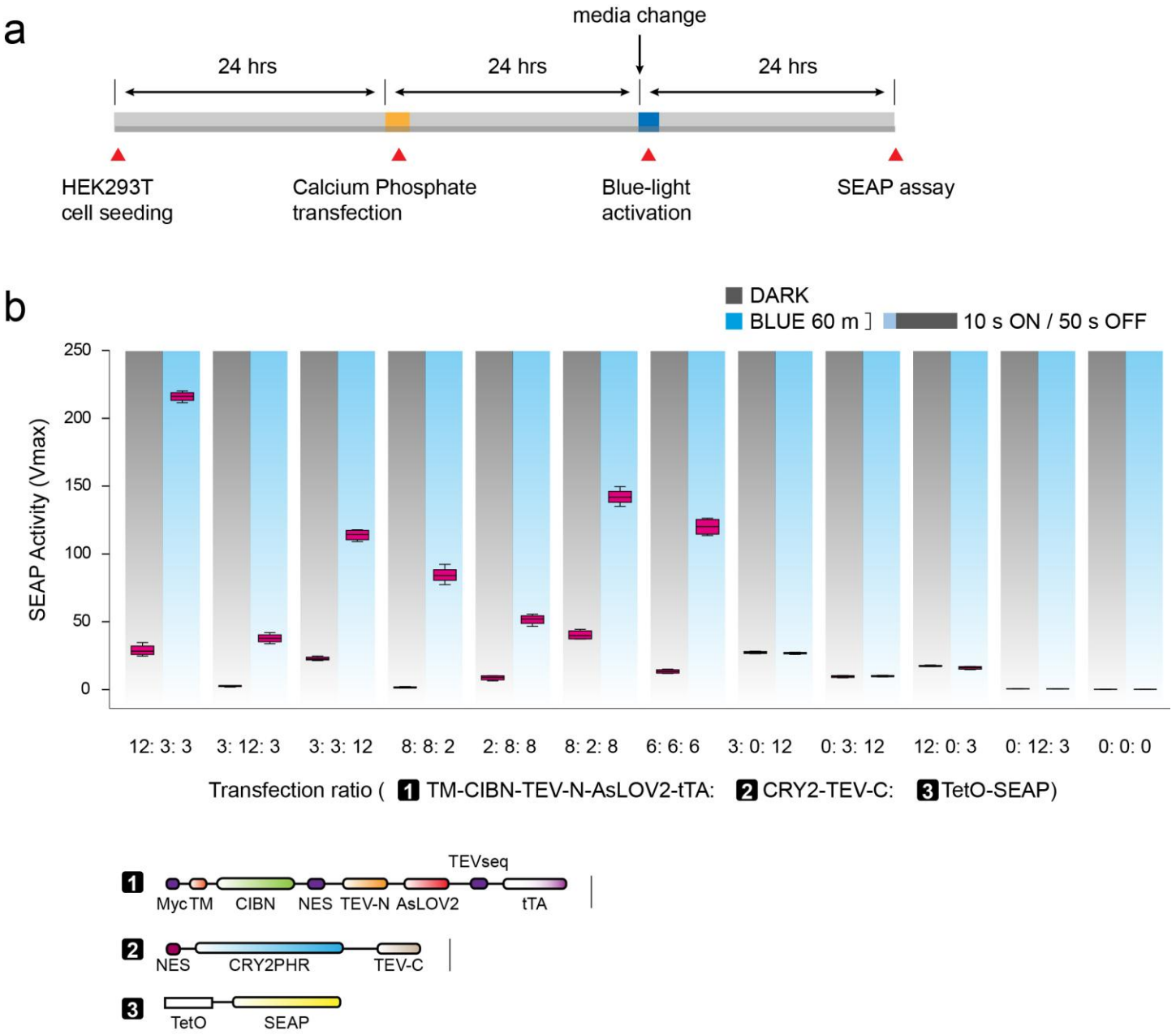

Supplementary Figure 2

Optimization of BLITz in various conditions of transfection ratios.

(a) Schematic experimental procedures in HEK293T cells. Right before blue light activation, media was replaced by fresh DMEM containing 10% FBS. (b) Summary graph of SEAP assay at different ratios of BLITz constructs. Notably, 8:8:2 (TM-CIBN-TEV-N-AsLOV2-tTA: CRY2-TEV-C: TetO-SEAP) ratio shows the best fold changes. Error bar represents ± S.D. of three independent experiments.

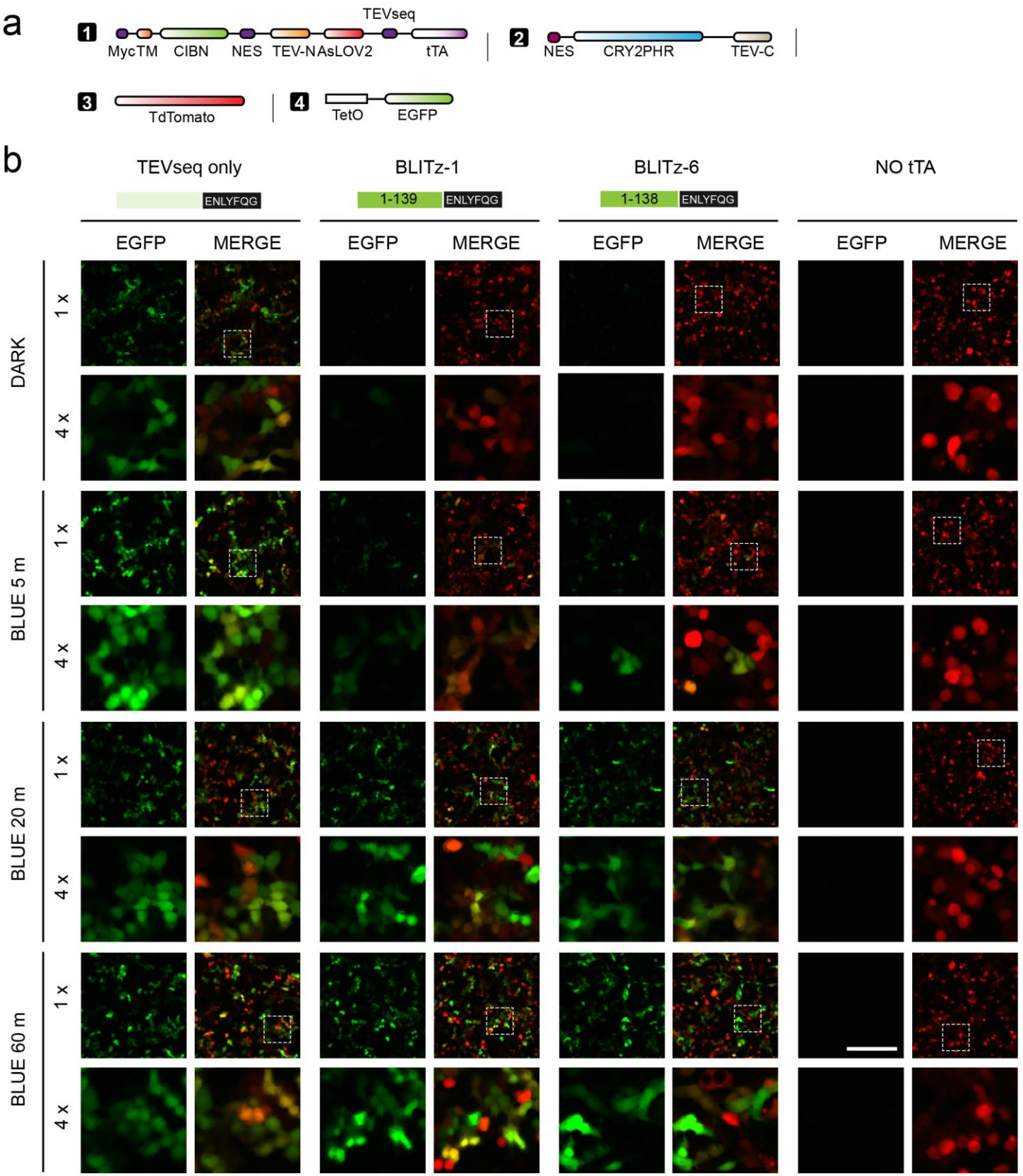

Supplementary Figure 3

Blue-light-dependent EGFP expression of BLITz in HEK293T.

(a) Schematic designs of DNA constructs. TdTomato was separately transfected for a transfection marker. (b) Representative images of gene expression by BLITz. Parts of images are same as Fig. 1b. Images at Blue light 5 min and 20 min are additionally supplemented. Dashed boxes were magnified (4x) for clarification. Expression pattern of EGFP are very similar to the pattern of SEAP assay (Fig. 1c). Scale bar, 200 μm (1x) and 50 μm (4x magnified images).

Nature Methods: doi:10.1038/nmeth.4234

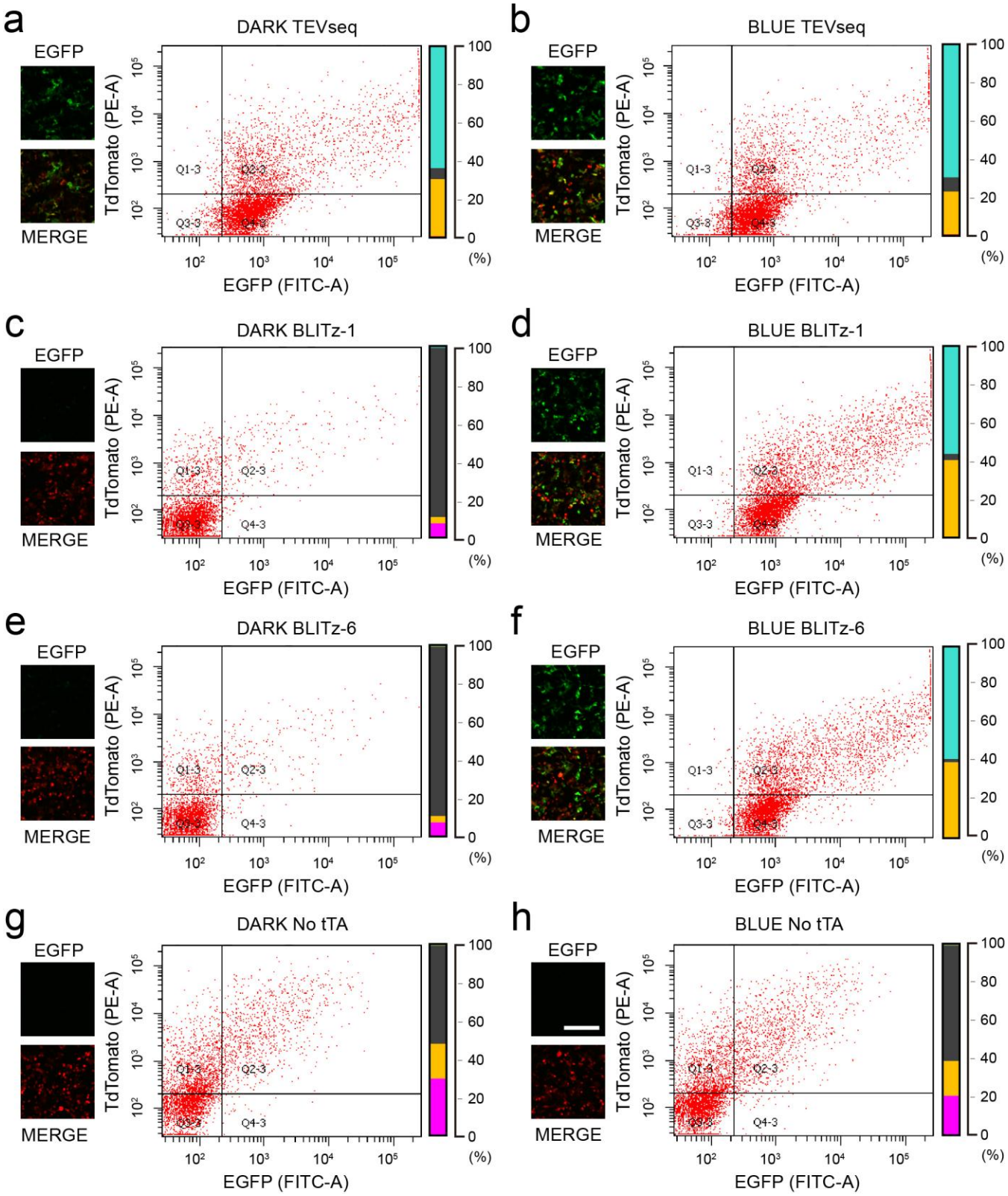

Supplementary Figure 4

Two-color flow cytometry analysis of EGFP reporter expression in the BLITz system.

(a-h) Scatter plots of two-color (y-axis: TdTomato, x-axis: EGFP) flow cytometry analysis in HEK293T transfected with BLITz systems. Analyzed cells were divided into four quadrants (Black, Magenta, Turquoise, and Yellow) by EGFP and TdTomato fluorescent intensity. Distribution of four quadrants are displayed as bar graph. The right upper quadrant suggests both high TdTomato and EGFP expression. Confocal images are same as Fig. 1b. Scale bar, 200 μm.

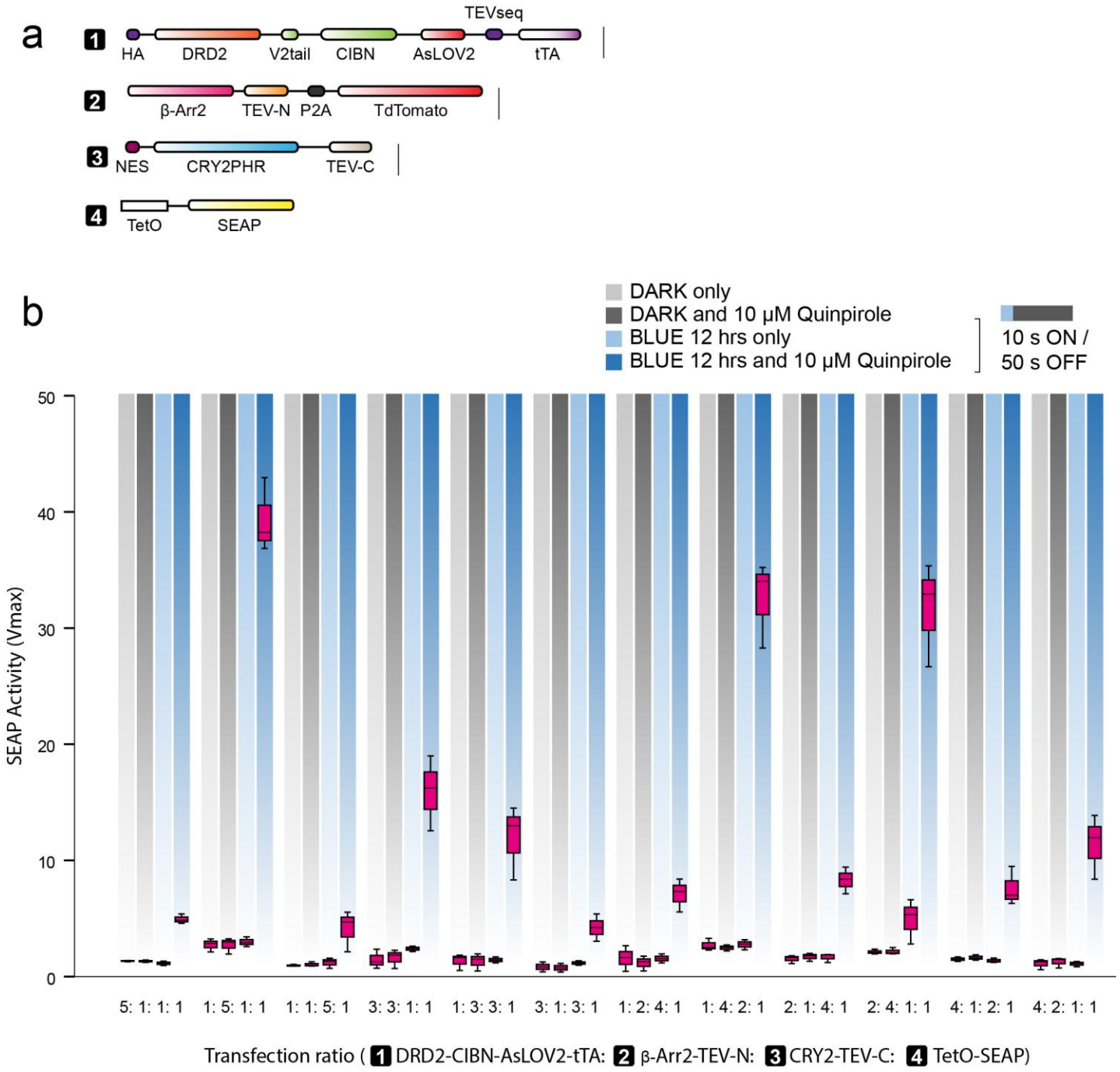

Supplementary Figure 5

Optimization of DRD2-iTango at various transfection ratios.

(a) Schematics of DNA constructs of DRD2-iTango. (b) SEAP assay shows different gene expression level of DRD2-iTango at various transfection ratios. To test DRD2-iTango, we treated 10 μM Quinpirole and shined 10-second pulsed blue light for 12 hrs. Note that whenever high ratio of β-Arrestin2-TEV-N was transfected, fold change of gene expression was higher. The summary graph is represented by means ± S.D. of three independent measurements.

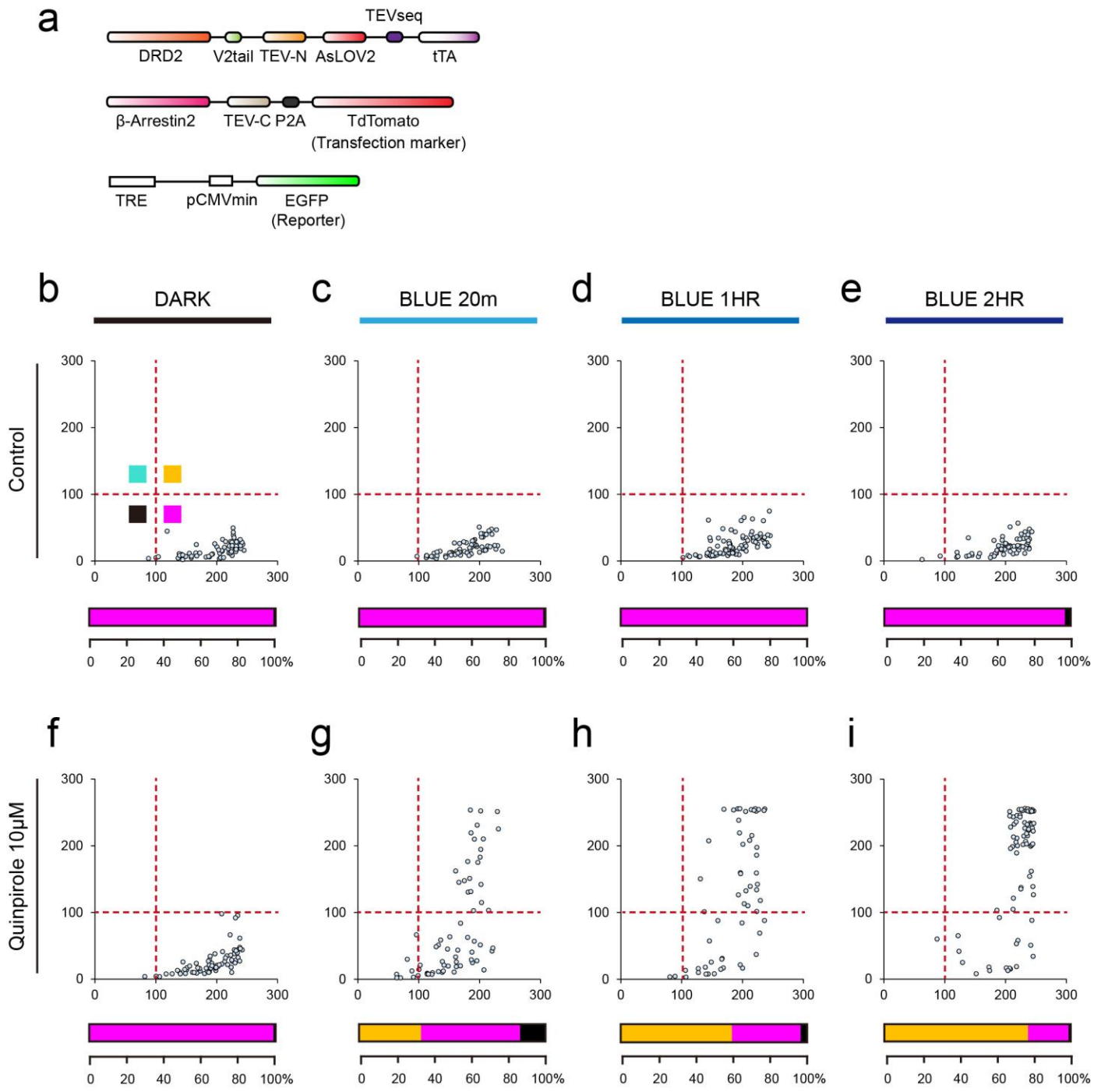

Supplementary Figure 6

Scatter-plot analysis of blue-light- and agonist-dependent EGFP expression in DRD2-iTango2.

(a) Schematics of DNA constructs of DRD2-iTango2. (b-i) Two-color scatter plots (x-axis: TdTomato, y-axis: EGFP) of hippocampal culture neuron expressing DRD2-iTango2. Analyzed cells were divided by four quadrants (Black, Magenta, Turquoise, and Yellow) and their distributional percentage was quantified by horizontal histograms. Red dot cross lines indicate threshold for defining four quadrants.

Nature Methods: doi:10.1038/nmeth.4234

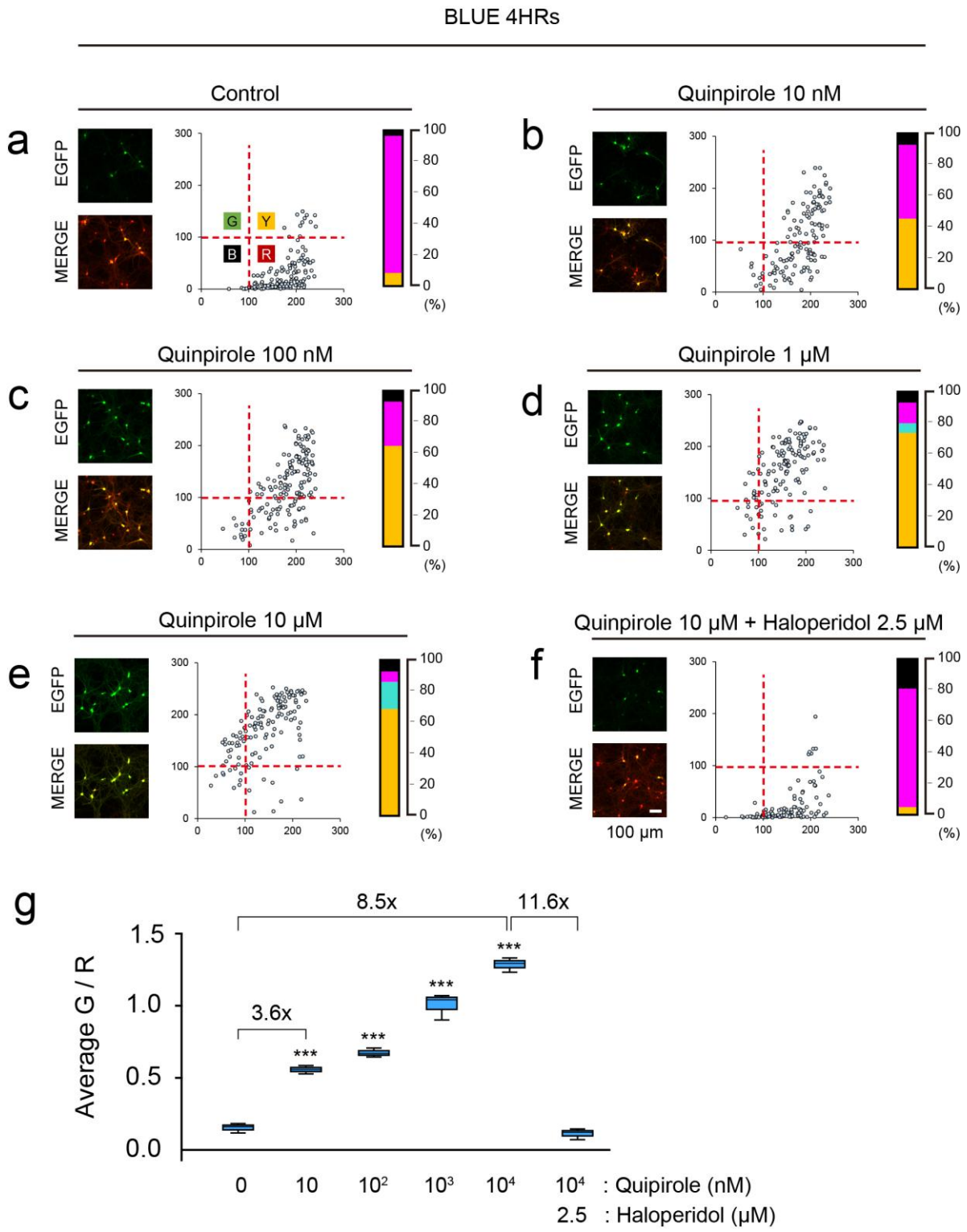

Supplementary Figure 7

Agonist dose-dependent expression of EGFP reporter in DRD2-iTango2.

(a-f) Representative confocal images (left panel), scatter plots of two-color (middle panel; y-axis: TdTomato, x-

axis: EGFP), and distribution graph (right panel) of DRD2-iTango2 with different concentration of quinpirole and haloperidol in blue light condition. Analyzed cells were divided by four quadrants (Black, Magenta, Turquoise, and Yellow) and their distributional percentage was displayed as vertical histograms. Red dot cross lines indicate threshold for defining four quadrants.Scale bar, 100 μm. (g) Summary graph of average G/R (Control: 0.15 ± 0.03, Quinpirole 10 nM: 0.55 ± 0.02, Quinpirole 100 nM: 0.67 ± 0.03, Quinpirole 1 μM: 1.00 ± 0.09, Quinpirole 10 μM: 1.28 ± 0.04, and Quinpirole 10 μM + Haloperidol 2.5 μM: 0.11 ± 0.03; 3 independent experiments, Mean ± S.E.M; oneway-ANOVA $p<0.001$; Bonferroni post-hoc test; ***$p < 0.001$) and fold changes.

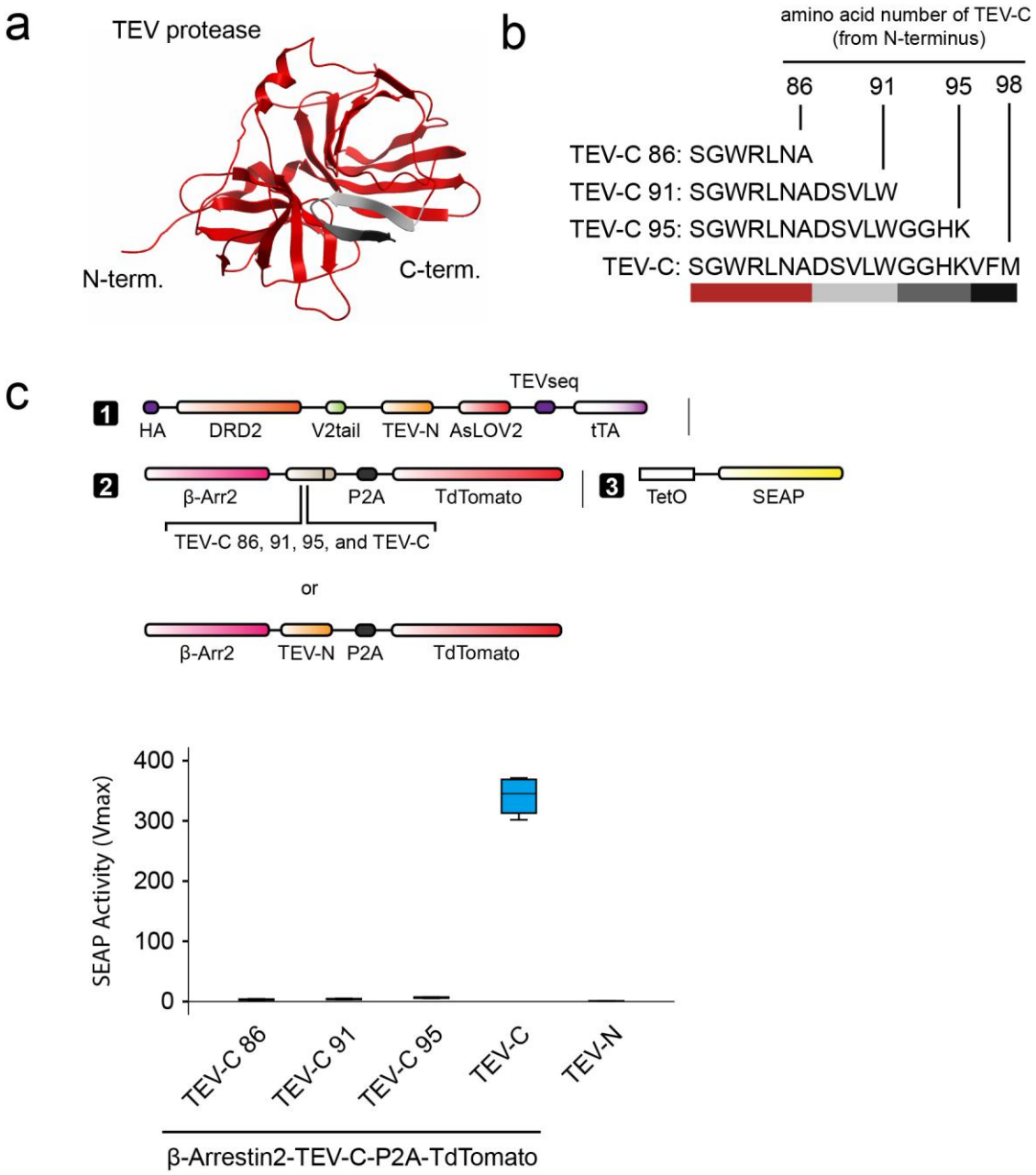

Supplementary Figure 8

Complete elimination of DRD2-iTango2 activity by further deletion of C-terminal amino acids of TEV-C.

(a, b) Schematic protein structure of full-length TEV protease and C-terminal amino acid sequences of deleted mutants of TEV-C (TEV-C 86, TEV-C 91, TEV-C 95; numbers indicate the position of last amino acid within the deleted mutant). To optimize the minimum sequence of TEV-C for DRD2-iTango2 system without losing intact protease activity, we generated three mutants of β-Arrestin2-TEV-C-P2A-TdTomato by deleting C-terminal amino acids of TEV-C. N-terminal intact region are colored with red and deleted region are colored with light gray, dark gray, and black. (c) Deleted iTango2 mutant constructs or TEV-N as control were transfected into HEK293T cells. After blue light (2 hrs) and 10 μM quinpirole treatment, SEAP activity was

measured to check the level of gene expression induced by TEV-protease-dependent cleavage. TEV protease function is completely abolished in three C-terminal deletion mutants (TEV-C 86: 3.08 ± 1.01, TEV-C 91: 3.96 ± 0.81, TEV-C 95: 6.45 ± 1.00) or TEV-N (0.88 ± 0.06), but remains in the original truncated version of TEV-C (340.87 ± 33.53). Mean ± S.D.

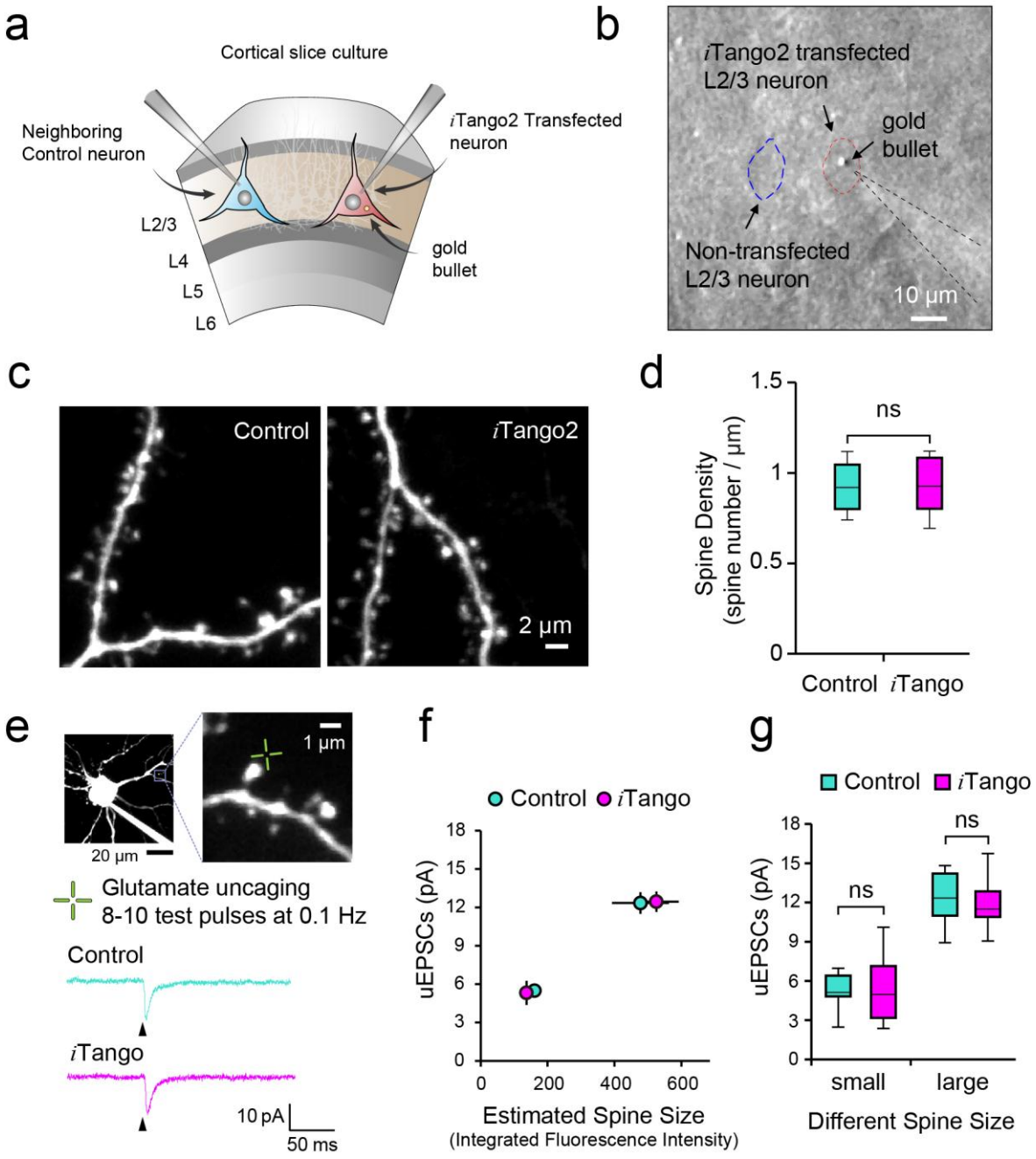

Supplementary Figure 9

No changes in excitatory-synapse numbers and functions by iTango2.

(a) Schematic drawing of experiments. Layer 2/3 pyramidal neurons with DRD2-iTango2 transfected or neighboring control neurons were compared. (b) iTango2 transfected neuron was identified by TdTomato signal originated from β-Arrestin2-TEV-C-P2A-TdTomato. In addition, gold particle was observed from DNA transfected neurons. (c) Representative images of dendritic spines from control and iTango2 transfected neurons. To visualize spine morphology clearly, Alexa-488 (200 μM) was added into the recording pipette. (d) Average graph of spine density (Control: 0.93 ± 0.07, 5 neurons, 2.8 ROI / neuron; iTango2: 0.94 ± 0.06, 8

neurons, 2.6 ROI / neuron, $p > 0.1$). (e) Target neuron image and dendritic spine for glutamate uncaging. Cross indicates glutamate uncaging spot. Representative traces of uncaging induced AMPAR-uEPSCs. Arrow indicates uncaging time. 2.5 mM MNI-Glutamate was perfused in normal ACSF. Spontaneous activity was blocked by 1 μM TTX. 1 ms pulse of 720 nm laser was used for glutamate photolysis. (f) Relationship between uEPSCs and spine size (Control with small size: 160.87 ± 9.23; iTango with small size: 136.94 ± 20.20, $p > 0.05$; Control with large size: 477.78 ± 85.1; iTango with large size: 525.50 ± 66.89, $p > 0.05$). (g) The amplitude of uEPSCs grouped by spine size was compared between control and iTango2 transfected neurons (Control: 3 neurons, 20 spines; iTango2: 6 neurons, 24 spines; Control with small size: 5.50 ± 0.39; iTango2 with small size: 5.31 ± 0.94, $p > 0.1$; Control with large size: 12.34 ± 0.84; iTango with large size: 12.44 ± 0.78, $p > 0.1$).

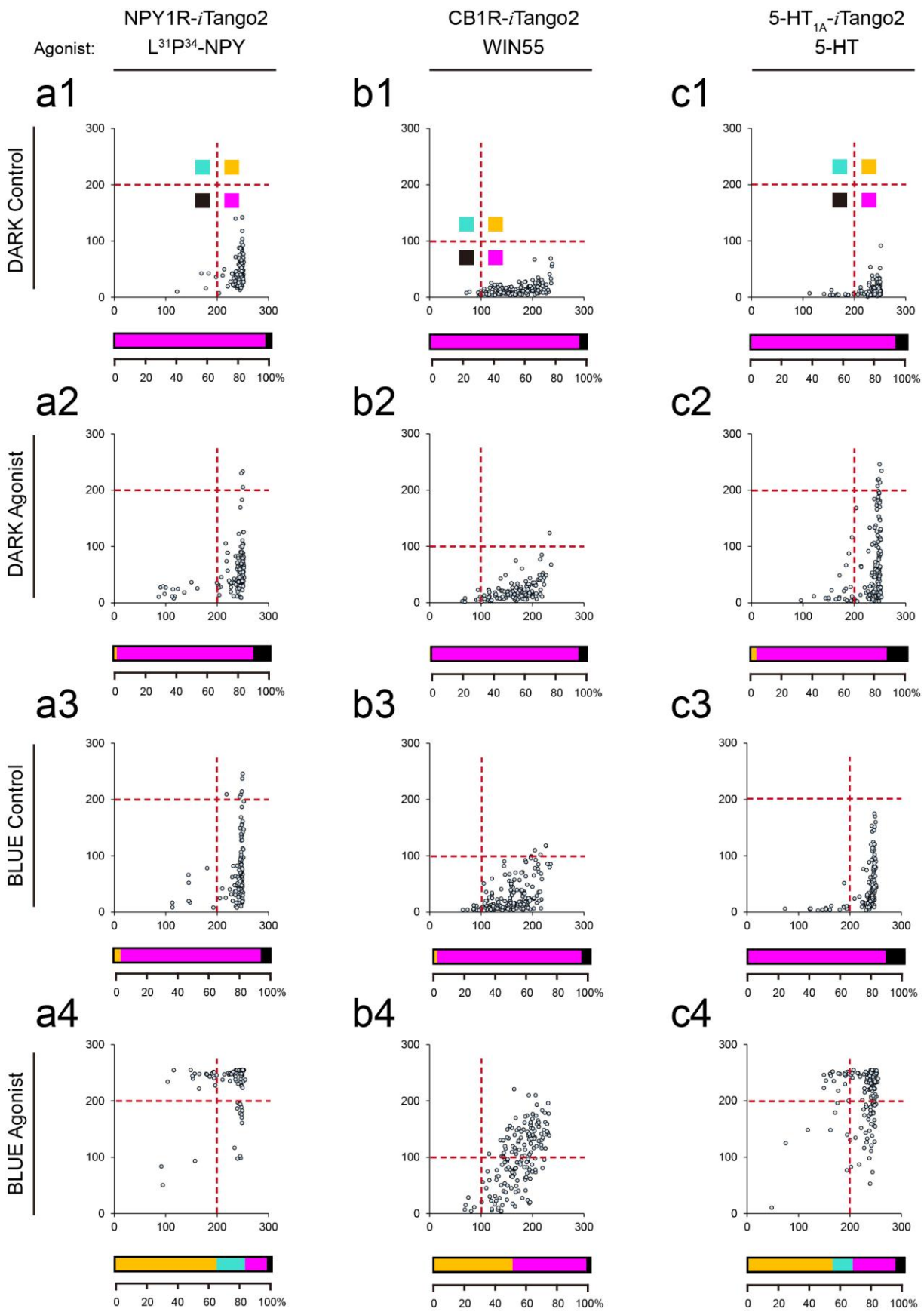

Nature Methods: doi:10.1038/nmeth.4234

Supplementary Figure 10

Scatter-plot analysis of NPY1R-iTango2, CB1R-iTango2, and 5-HT1A-iTango2.

(a1-4) Scatter plots (x-axis: TdTomato, y-axis: EGFP) of hippocampal culture neuron expressing NPY1R-iTango2. (b1-4) Scatter plots of CB1R-iTango2. (c1-4) Scatter plots of 5-HT1A-iTango2. Analyzed cells were divided by four quadrants (Black, Magenta, Turquoise, and Yellow) and their distributional percentage was quantified by horizontal histograms. The right upper quadrant (Yellow) represents both high TdTomato and EGFP expression. Red dot cross lines indicate threshold for defining four quadrants.

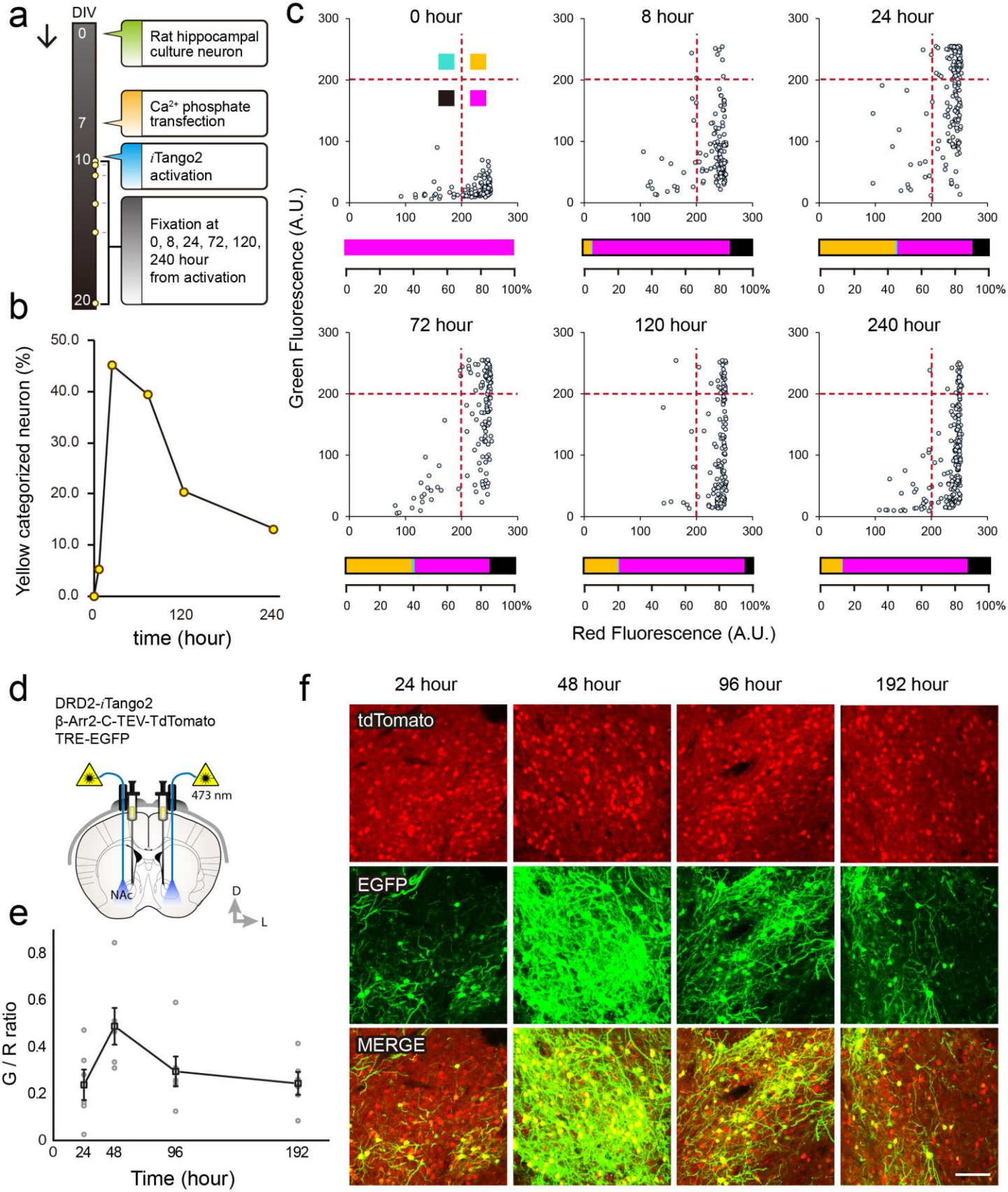

Nature Methods: doi:10.1038/nmeth.4234

Supplementary Figure 11

Time course of iTango2 reporter-gene expression *in vitro* and *in vivo*.

(a) Experimental time line of DRD2-iTango2 in hippocampal culture neurons. (b) Percentage change of Yellow categorized neurons over time (upper right quadrant). (c) Two-color scatter plots (x-axis: TdTomato, y-axis: EGFP) of DRD2-iTango2. Analyzed cells were divided by four categories (Turquoise, Yellow, Black, and Magenta). Division of categories is indicated as red dot cross lines. Total cell numbers of each group are as following: (0 hour: 138 neurons, 8 hour: 137 neurons, 24 hour: 173 neurons, 72 hour: 133 neurons, 120 hour: 152 neurons, 240 hour: 208 neurons). (d) Schematic figure of virus injection. (e) Summary graph of G/R ratio changes after induction of DRD2-iTango labeling (24 hour: 0.238 ± 0.065, 6 mice; 48 hour: 0.489 ± 0.079, 6 mice; 96 hour: 0.295 ± 0.064, 6 mice; 192 hour: 0.244 ± 0.049, 6 mice; $F_{hour} = 3.32$, $p < 0.05$). (f) Coronal sections of the NAc respectively from left to right imaged 24, 48, 96, and 192 hour after induction of iTango2 labeling. Scale bar, 100 μm.

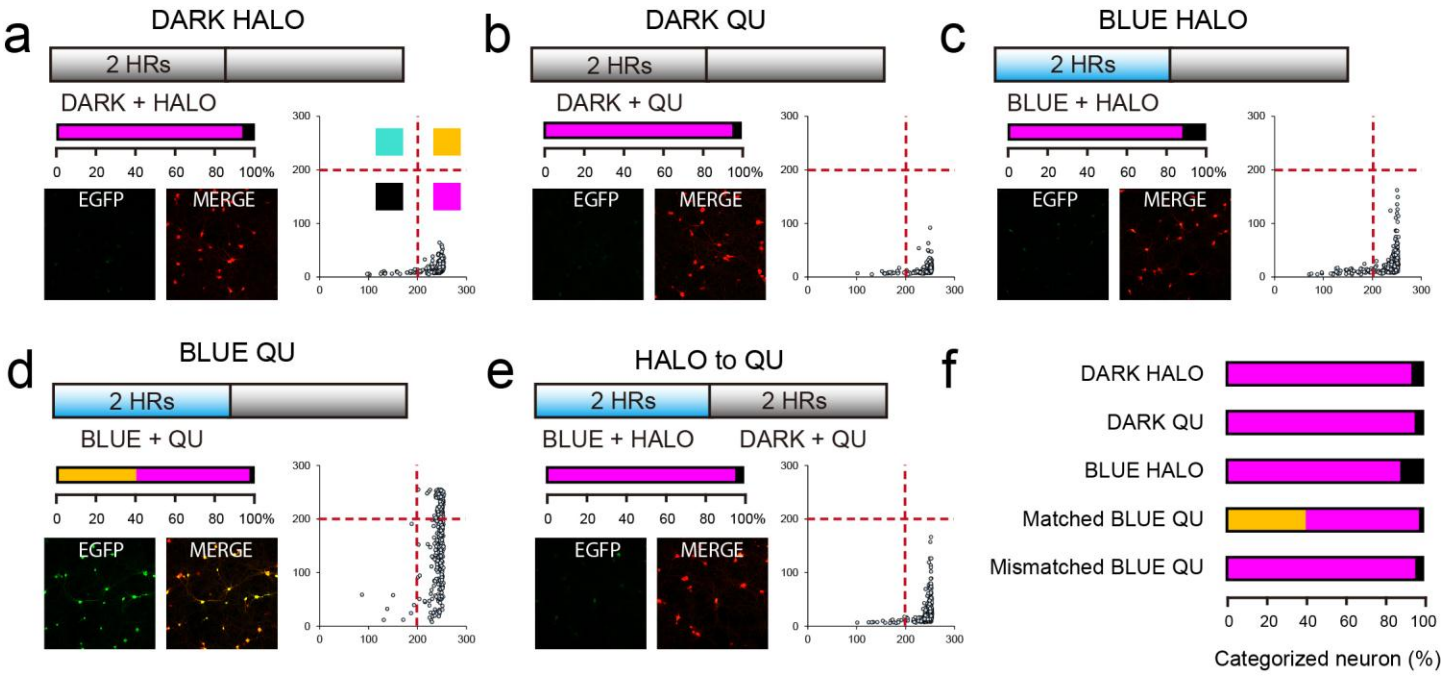

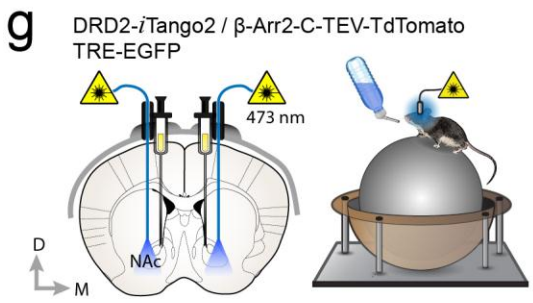

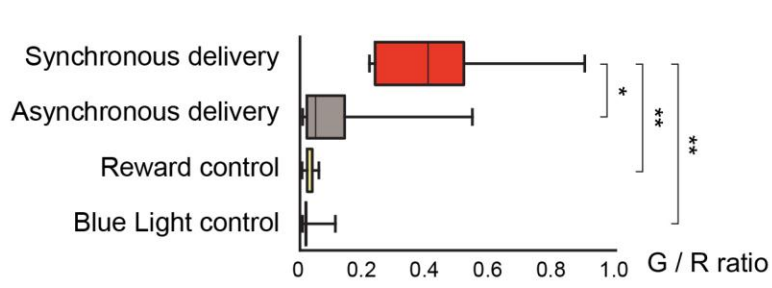

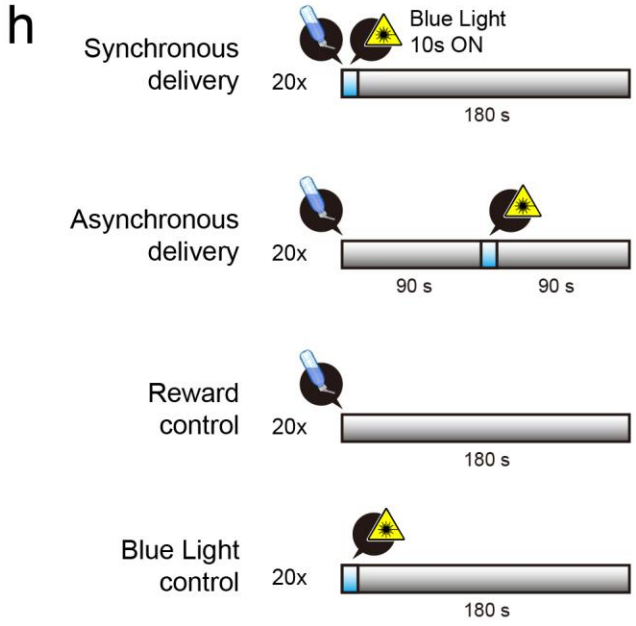

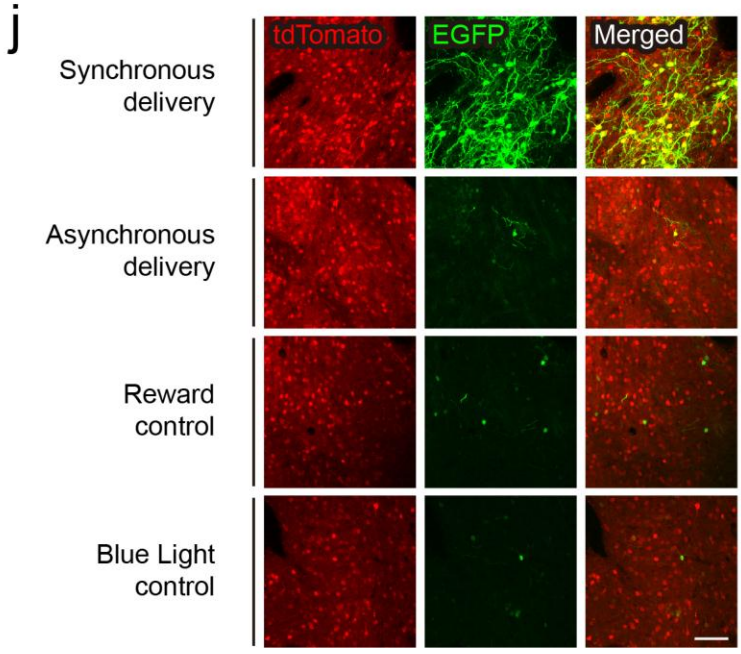

Nature Methods: doi:10.1038/nmeth.4234

Supplementary Figure 12

Time offset analysis of DRD2-iTango2 labeling.

(a-e) Schematics represent experimental design of in vitro time offset experiment. Representative images (left panel) and scatter plots (right panel, y axis: EGFP, x axis: TdTomato) of EGFP expression in time offset experiment of iTango2. (f) Analyzed cells were divided by four quadrants (Black, Magenta, Turquoise, and Yellow) and their distributional percentage was displayed as horizontal histograms. (g) Schematic figures of virus injection and experiment setup. (h) Schematic of experiment; (1) blue light in sync with reward, (2) blue light out of sync with reward, (3) reward alone, or (4) blue light alone was administered to induce the expression of EGFP reporter. (i) Summary graph of G/R ratio in NAc (Synchronous delivery: 0.446 ± 0.104, 6 mice; Asynchronous delivery: 0.135 ± 0.084, 6 mice; Reward control: 0.034 ± 0.007, 6 mice; Blue light control: 0.035 ± 0.019, 6 mice; *$p < 0.05$, **$p < 0.01$). (j) Coronal sections of the NAc from mice treated with synchronous delivery, asynchronous delivery, reward alone, or blue light alone, respectively from top to bottom. Scale bar, 100 μm.

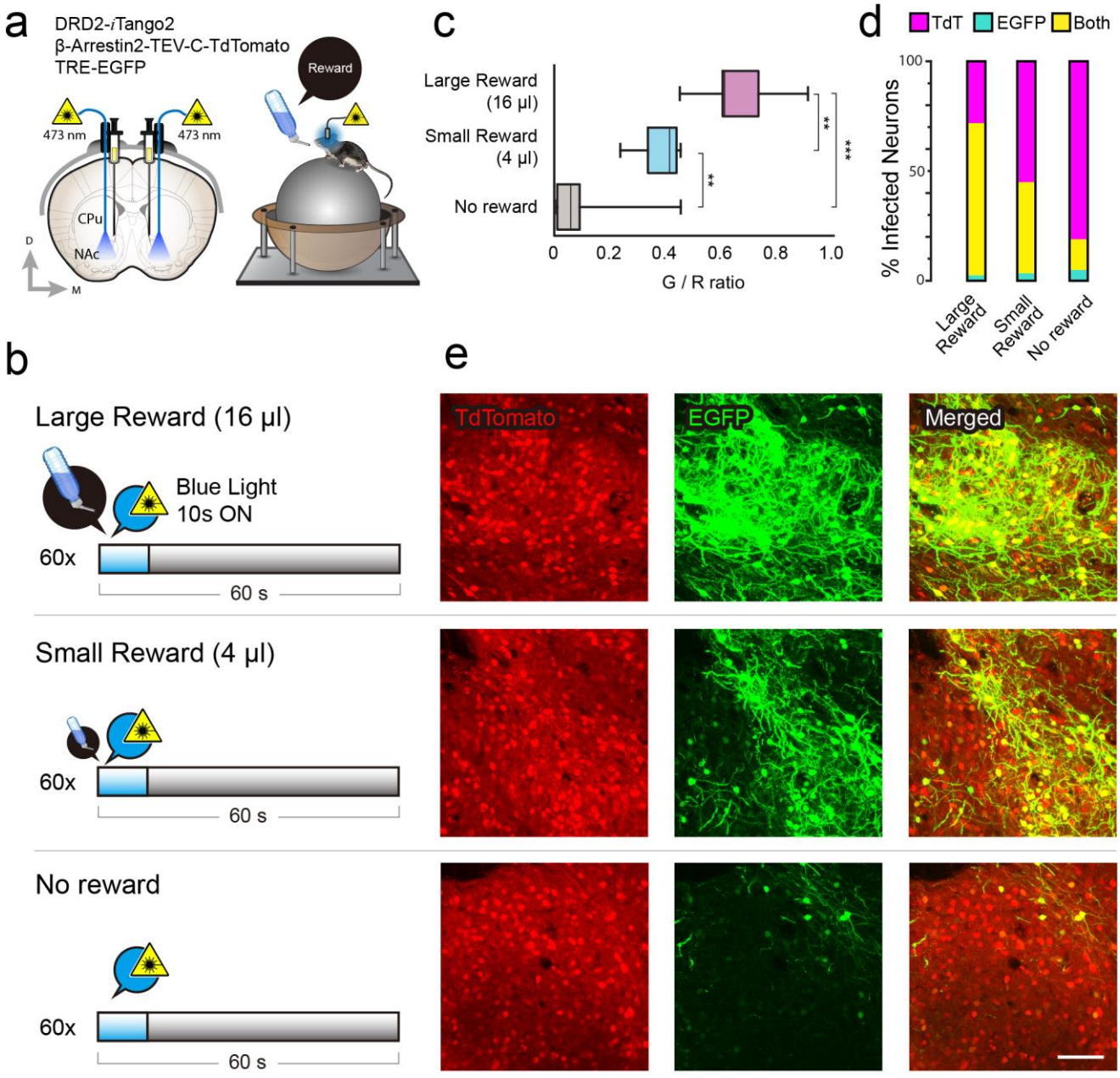

Supplementary Figure 13

In vivo reward-amount-dependent iTango2 labeling in the NAc.

(a) Schematic figures of virus injection and experiment setup. (b) Schematic of experiment; blue light was administered in sync with different amounts of reward (large reward: 16 µl, small reward: 4 µl, or no reward) to induce the expression of EGFP reporter. (c) Summary graph of G/R ratio in NAc (Large reward: 0.662 ± 0.070, 5 mice; Small reward: 0.382 ± 0.033, 6 mice; No reward: 0.114 ± 0.070, 6 mice; **p < 0.01, ***p < 0.001). (d) Quantification of infected neurons expressing tdTomato alone, EGFP alone, or co-expressing both fluorescent proteins. (e) Coronal sections of the NAc from mice receiving large reward (top), small reward (middle), or no reward (bottom). Scale bar, 100 µm.

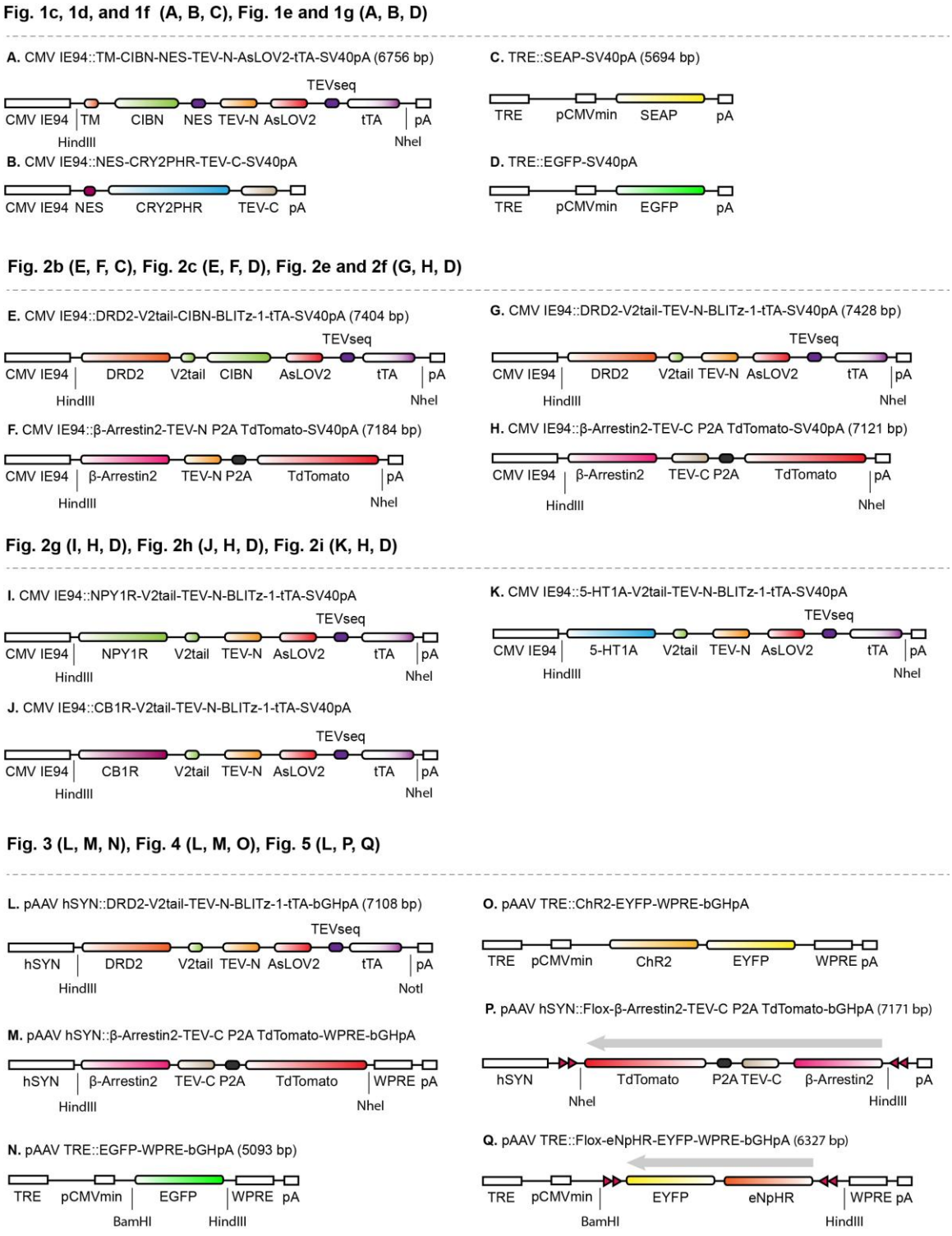

Supplementary Figure 14

Schematic domain structures of constructs used in this study.